



HAL
open science

Synthesis of latex stabilized by unmodified cellulose nanocrystals: the effect of monomers on particle size

Clara Jimenez Saelices, Maud Save, Isabelle Capron

► **To cite this version:**

Clara Jimenez Saelices, Maud Save, Isabelle Capron. Synthesis of latex stabilized by unmodified cellulose nanocrystals: the effect of monomers on particle size. *Polymer Chemistry*, 2019, 10 (6), pp.727-737. 10.1039/c8py01575a . hal-01987494

HAL Id: hal-01987494

<https://hal.science/hal-01987494v1>

Submitted on 27 Oct 2020

HAL is a multi-disciplinary open access archive for the deposit and dissemination of scientific research documents, whether they are published or not. The documents may come from teaching and research institutions in France or abroad, or from public or private research centers.

L'archive ouverte pluridisciplinaire **HAL**, est destinée au dépôt et à la diffusion de documents scientifiques de niveau recherche, publiés ou non, émanant des établissements d'enseignement et de recherche français ou étrangers, des laboratoires publics ou privés.



Synthesis of Latex Stabilized by Unmodified Cellulose Nanocrystals: Role of Monomers on Particle Size

Clara Jiménez Saelices,^a Maud Save^b and Isabelle Capron^{*a}

Received 00th January 20xx,
Accepted 00th January 20xx

DOI: 10.1039/x0xx00000x

www.rsc.org/

Cellulose nanocrystals (CNCs) are sustainable rod-shaped nanoparticles able to adsorb at oil-water interfaces to produce highly stable Pickering emulsions with enhanced mechanical properties. Polymerization of the CNC-stabilized monomer droplets is investigated in details to elucidate the synthesis mechanism of both micro- and nanoparticles of latex in relationship with the initial sizes of the droplets. It is shown in this study that unmodified CNCs, used as sole stabilizer, are efficient to produce both monomer-in-water Pickering emulsion and nanocomposite latex particles with controlled dimensions. For the initial liquid emulsion of styrene, two populations of droplets were observed: micrometric droplets with diameters that decrease down to 5 μm with increasing CNC concentrations, and nanometric droplets with a diameter distribution ranging from 500 nm to 2 μm for all CNC concentrations. It leads to two distinct populations of polystyrene latex particles by polymerization in aqueous dispersed media, i.e. microparticles of 5–18 μm and nanoparticles with an average diameter below 1 μm . The polymerization of various monomers, i.e. styrene, lauryl methacrylate, isobornyl Acrylate, butyl methacrylate, methyl methacrylate, in the presence of different initiators highlighted that the solubility of the monomer in the aqueous continuous phase is the key parameter to tune the size distribution of the latex particles. Nanocomposite CNC-stabilized waterborne latexes were prepared from polymer with different glass transition temperatures.

Introduction

Cellulose is the most widespread biopolymer on earth. It is present in a wide variety of plants where it mainly acts as a reinforcement material. The supramolecular structure of this polysaccharide is not uniform. Cellulose contains both crystalline phases and disordered domains that are generally considered to be amorphous. These amorphous regions are considered to be structural defects in the microfibrils and can be removed by acid hydrolysis to prepare highly crystalline particles called cellulose nanocrystals (CNCs). Sulfuric acid hydrolysis is typically used to isolate CNCs;¹ grafting anionic sulfate half ester groups (OSO_3^-), the negative charges at the surface are responsible for colloidal stability in water by electrostatic repulsion.^{2–8} CNCs from wood are rigid, rod-shaped nanoparticles with a length of 150–200 nm and a width of 3–20 nm.⁹ They are associated with a very high aspect ratio (around 30), high axial elastic modulus (150 GPa), high specific surface (200–300 m^2g^{-1}) and low density (1.6 $\text{g}\cdot\text{cm}^{-3}$).^{10–12} CNCs are renewable and toxicity studies have shown them to be harmless.¹³ In recent years there has been a growing interest to combine the outstanding properties of CNCs produced from

renewable resources with the properties of synthetic polymers.^{14, 15}

The colloidal dispersions of submicronic polymer particles produced by polymerization in aqueous dispersed media are known as waterborne latex particles. Waterborne latexes are used in many applications, including adhesives, paints, paper coating, printing inks, rubber products, cement reinforcement, as well as in medical industry.^{16–18} They can be produced by different heterophase polymerization processes like emulsion polymerization, miniemulsion polymerization, dispersion polymerization or suspension polymerization.^{19–21} From an engineering viewpoint, a water-based continuous phase favors heat transfer of the exothermic polymerization reaction and facilitates polymer recovery from the reactor as a fluid aqueous colloidal dispersion. The process is also environmentally benign, meeting one of the green chemistry requirements concerning the decrease of volatile organic compounds (VOC's). Emulsion polymerization commonly involves the use of surfactants or polar co-monomers to stabilize the growing polymer particles and to prevent the monomer droplets from coalescence. However, excess surfactants can have a negative impact on the material properties and the environment because they remain in the latex after polymerization. To limit this drawback, polymer scientists have investigated surfactant-free emulsion polymerization, where the charges of the initiator or co-monomer play the role of a stabilizer.^{22–24} Nonetheless, the low solid content is a limitation of these techniques. Molecular surfactants have also been replaced with macromonomers or amphiphilic copolymers,^{25–29} but the high number of steps required for the synthesis of these stabilizing polymers is a

^a UR 1268 Biopolymères Interactions Assemblages, INRA, 44316 Nantes, France.

E-mail: Isabelle.capron@inra.fr

^b CNRS, University Pau & Pays Adour, E2S UPPA, Institut des Sciences Analytiques et de Physico-Chimie pour l'Environnement et les Matériaux, IPREM, UMR5254, 64000, PAU, France.

† Electronic Supplementary Information (ESI) available. See DOI: 10.1039/x0xx00000x

limitation for such systems. Since the early studies carried out at the beginning of the 2000s,^{30, 31} the use of reactive hydrophilic polymers able to simultaneously act as both control agents and macroinitiators or macromolecular chain transfer agents proved to be very efficient to produce stable monodispersed latex particles via surfactant-free emulsion or dispersion polymerization.³²⁻³⁵ A wide variety of synthetic and biosourced hydrophilic reactive polymers have been investigated for the synthesis of polymer colloids with various morphologies by polymerization-induced self-assembly (PISA), including functionalized polysaccharides that have proved to be efficient reactive stabilizers.³⁶⁻³⁸

Another promising alternative for replacing molecular surfactants is to use colloidal particles as stabilizers. Amphiphilic particles can be used to stabilize emulsion droplets, creating the so-called Pickering emulsions.^{39, 40} Compared to conventional emulsions, a low fraction of colloidal particles is required to produce Pickering emulsions with higher stability because the adsorption energy is several orders larger than with surfactants.⁴¹ Colloidal particles form a solid armor around the droplet that avoids their coalescence by steric repulsion. A large variety of nanoparticles has been successfully used to stabilize emulsion droplets and generate nanocomposite latex via different heterophase polymerization techniques.^{35, 42} Silica, Laponite clay, magnetite, zinc oxide, titanium and graphene oxide are examples of commercially-available inorganic nanoparticles used in Pickering emulsions.⁴³⁻⁴⁸ There has been a growing interest in recent years in the use of biobased nanocelluloses as Pickering emulsifiers.⁴⁹⁻⁵³ It has been shown that CNCs can effectively stabilize oil-water interfaces by strong adsorption along the less polar (200) crystalline plane.⁵⁴ CNCs have been incorporated into polymerization processes to design nanocomposite latexes in order to improve the mechanical properties of the polymer.⁵⁵

In the early studies, CNCs were used in combination with surfactants and were anchored at the interface either by coupling agents⁵⁶⁻⁵⁸ or by electrostatic interactions with surfactants.^{59, 60} CNCs were therefore not directly involved in the stabilization of monomer droplets or latex particles. Recent studies have shown that modified CNCs can be used to stabilize latexes. For example, heterogeneously modified CNCs with hydrophobic alkyl chains were used to stabilize polystyrene (PS) latex with micrometric diameters.⁶¹ Kedzior *et al.* produced CNC nanocomposite latexes with a double morphology composed of micrometric polymer particles decorated with nanometric ones.⁶² They used methyl-cellulose (MC)-coated CNCs to stabilize poly(methyl methacrylate) (PMMA) latex particles via microsuspension polymerization. The presence of polymer nanoparticles was explained by the excess of methyl cellulose chains, which implies the stabilization by methyl cellulose alone. Zhang *et al.* used CNCs hydrophobically modified with different alkyl-amines to stabilize emulsions with droplet sizes of only a few hundred nanometers, leading to nanometric latexes by polymerization of styrene.⁶³ Using acetylated CNCs, Werner *et al.* showed that polymerization of styrene in aqueous dispersed media produced a mixture of micrometric and nanometric

polystyrene latex particles from an initial liquid emulsion composed of droplets in the micrometer range.⁶⁴

This study presents for the first time the use of unmodified CNCs as the sole stabilizer of both monomer-in-water Pickering emulsions and final nanocomposite latex particles synthesized by polymerization in aqueous dispersed media. In order to shed light on the production of stable latex particles of different sizes (latex microparticles and latex nanoparticles), we investigated in detail the emulsification and polymerization processes according to various experimental parameters. We first studied the surface charge of CNCs and the viscosity ratio between continuous and dispersed phases. Subsequently, a range of monomers (and initiators) with various limits of solubility in water were used to investigate the role of monomers on the droplet size and on the nucleation and growth of latex particles. A novel range CNC-based nanocomposite waterborne latex is targeted with polymers of a wide range of glass transition temperatures.

Experimental Section

Materials. The cotton cellulose nanocrystals (CNCs) were obtained from Whatman filters (grade 20 Chr). Commercial CNCs (c-CNCs) were provided by the University of Maine (Orono, ME, USA) in the form of aqueous suspensions at 12 wt%. c-CNCs were diluted, sonicated and intensively dialyzed for ten days before use. Hexadecane and the initiators, azobisisobutyronitrile (AIBN) and 4,4'-Azobis(4-cyanovaleric acid) (ACPA), were acquired from Sigma Aldrich and used without further purification. The monomers (Styrene (S), Lauryl Methacrylate (LMA), Isobornyl Acrylate (iBoA), Butyl Methacrylate (BMA), Methyl Methacrylate (MMA)) were provided by Sigma Aldrich (> 99%) and were passed through an alumina column before use to remove the inhibitors. Table S1 shows the density, solubility in water, viscosity and surface tension of the selected monomers. Water was purified with the Milli-Q reagent system (18.2 M Ω cm Millipore Milli-Q purification system).

CNC preparation. Cellulose nanocrystals (CNCs) were prepared from cotton linters according to the method of Revol *et al.*⁵ with minor modifications. Briefly,⁵⁰ 25 g of filters were dispersed in water and then hydrolyzed with sulfuric acid at 58% at 70°C under stirring for 20 min. After hydrolysis, the suspension was washed by centrifugation, dialyzed to neutrality against Milli-Q water for 2 weeks, and deionized using mixed bed resin (TMD-8, Sigma Aldrich). The final dispersion was sonicated for 10 min, filtered through a 0.45 μ m filter, and stored at 4°C.

CNC characterization. The CNCs and the c-CNCs were visualized by Transmission Electron Microscopy (TEM) using a JEOL JEM-1230 TEM at 80 kV. The suspensions were deposited on a freshly glow-discharged carbon-coated copper grid (Electron Microscopy Sciences, UK) and negative staining was performed using phosphotungstic acid (1% w/v, adjusted to pH 6 with NaOH and filtered at 0.1 μ m). The grids were dried at room temperature. The average length and width of the nanocelluloses were analyzed from 100 images using Image J (Figure 1).

The surface charge density of CNCs and c-CNCs was measured by conductometric titration using an automated Metrohm 905 Titrando controlled by a computer with TIAMO software (Metrohm, Switzerland). The sulfate contents of suspensions (Figure 1) were titrated with NaOH. The degree of substitution of sulfate groups was calculated on the basis of the following equation:

$$d_s = (V_{eq} \cdot C_{NaOH} \cdot M_w) / m$$

where V_{eq} is the volume of NaOH in mL at the equivalent point, C_{NaOH} is the concentration (mol/L), M_w is the molar mass and m is the weight of titrated cellulose. The surface charge density was calculated by dividing the degree of substitution by the surface area of CNC.

	Origin	Lateral Size	Length	Surface Charge
CNC	Cotton	3 – 6 nm	50 – 250 nm	0.34 e nm^{-2}
c-CNC	Wood	4 – 16 nm	50 – 250 nm	0.60 e nm^{-2}

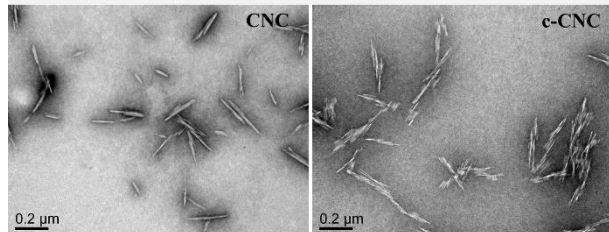


Figure 1. CNC Characterization

Emulsion and latex preparation and characterization

The Pickering emulsions were prepared by mixing an aqueous dispersion of CNCs and an organic phase at a 10/90 O/W volume fraction. For all the emulsions, the aqueous phase with 50 mM NaCl consisted of CNCs dispersed at concentrations between 0.2 and 2.3 wt% based on the styrene. This ionic strength was chosen to limit repulsions due to charged groups present at the surface. An oil soluble initiator (AIBN) was added to the monomer phase before emulsification (ratio: 100:1 w/w). When required, a water soluble initiator (ACPA) was also added to the aqueous phase before emulsification (50:50 molar fractions of both initiators). The emulsions were prepared by sonication with an ultrasonic device with a dipping titanium probe close to the surface (amplitude 2 corresponds to 4 W/mL applied power) for 45 s, using intermittent pulses. The resulting emulsion was polymerized at 70°C without stirring for 48 h. The kinetics of polymerization for monomers used in this work is shown in Figure S1.

At low CNC concentrations, the emulsions require a stabilization time before polymerization. If the polymerization is carried out before the stabilization of the droplets, neckless-like aggregates of droplets that polymerize during the coalescence stage are obtained (Figure S2). The emulsions were systematically kept for 48 hours in order to polymerize stable emulsions. In the case of emulsions prepared with high concentrations of CNC, this stabilization time does not affect the droplet diameters (Figure S3) and remains constant for months at 20°C.

The average droplet diameters and diameter distribution before polymerization, and the average polymer particle size and size distribution after polymerization were measured by laser light scattering particle size analysis using a Horiba LA-960

(Kyoto, Japan). Calibration with water was carried out before each measurement. The diameter was expressed as the surface mean diameter $D(3,2)$ (the Sauter diameter).

The emulsions were all visualized by transmission optical microscopy (BX51 Olympus microscope). Image analysis was used to measure the droplet diameters of the styrene-in-water emulsions. The number average droplet diameter, D_n , of the emulsions was measured from the microscopic images using ImageJ software.

Scanning electron microscopy (SEM) was used in order to visualize the formed latex. When there was more than one particle population, the latex dispersion was centrifuged several times for 2 min at 10000 g in order to separate the populations. The dried polymer particles were metallized with gold and visualized with a JEOL 6400F instrument.

Results and Discussion

Synthesis of polystyrene latex stabilized by cellulose nanocrystals: characterization of the initial emulsion and final polymer particles

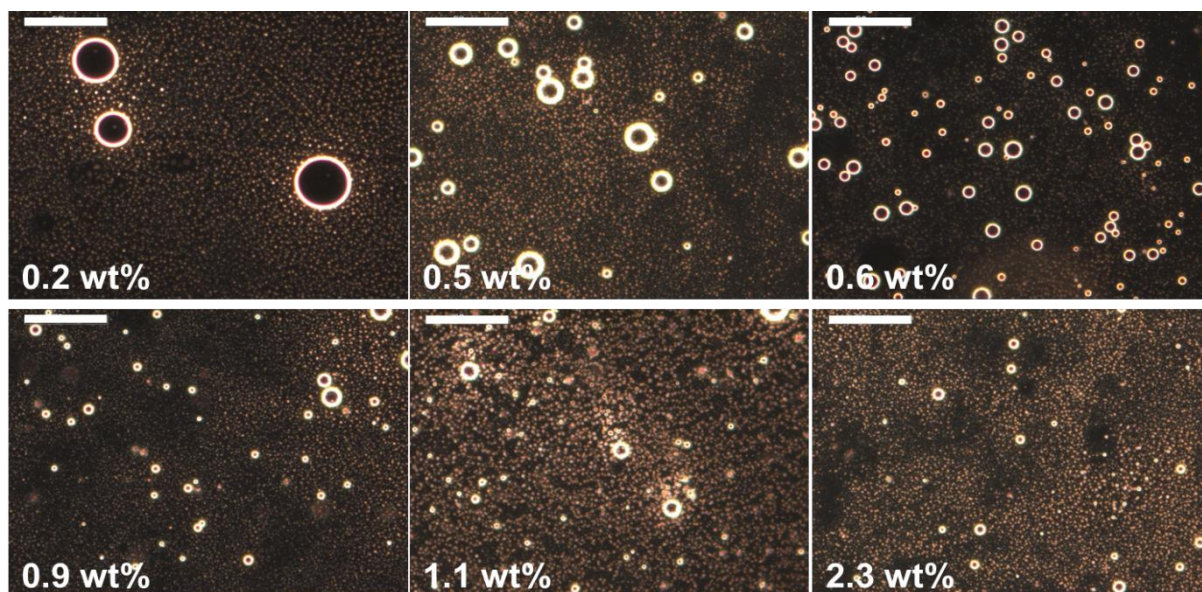


Figure 2 Optical microscopy images of styrene-in-water emulsions before polymerization showing two populations of droplets. The scale bar is 50 μm .

The CNC-stabilized Pickering emulsions were prepared using an aqueous suspension of CNC at concentrations between 0.2 and 2.3 wt%, based on the styrene. The transmission optical micrographs of styrene-in-water emulsions stabilized with increasing concentrations of CNCs are shown in Figure 2. For all emulsions, two very distinct populations of droplets were observed: droplets with diameters greater than 1 μm , and droplets with diameters smaller than 1 μm (Figure 2). For the purpose of clarity, the term ‘micrometric droplet’ is used in this study for droplets with diameters greater than 1 μm , whereas the term ‘nanometric droplet’ describes droplets with diameters of less than 1 μm . Micrometric droplet size decreases with increasing CNC concentration. This concentration dependence on the diameter, previously reported for hexadecane-in-water emulsions,⁵⁰ is known as the principle of limited coalescence.⁶⁵ The micrometric droplet diameter is then controlled by the amount of CNC. Regarding nanometric droplets, no dependence of the concentration on the diameter was observed. The average droplet diameter (D_n) of the styrene nanometric droplets was approximately 600 nm for all the emulsions, regardless of CNC concentration (Figure S4). Moreover, the nanometric droplets seem to be predominant compared to the micrometric droplets and represent a non-negligible volume (Figure 2).

Photographs of the emulsions before and after polymerization are shown in Figure 3. Before polymerization (Figure 3a), styrene micrometric droplets cream because styrene density ($d = 0.906 \text{ g}\cdot\text{cm}^{-3}$) is lower than water. Moreover, an increasing volume of cream is clearly observed by increasing the CNC concentration, whereas the initial volume of styrene is unchanged. Increasing the amount of CNCs allows the stabilization of a larger interface. Consequently, a greater number of smaller size droplets are formed, filling a larger emulsion volume. In addition, since CNCs are surrounded by a layer of water, it leads to more hydration layers, thus

immobilizing more water between the droplets. These two phenomena result in an increase in the cream volume with the concentration of CNCs (Figure 3a).^{50, 66} For all concentrations, the aqueous phase located below the creaming layer has a cloudy optical aspect, even after centrifugation. This is due to the presence of the nanometric droplets of styrene visualized by optical microscopy (Figure 2) that are not submitted to gravity.

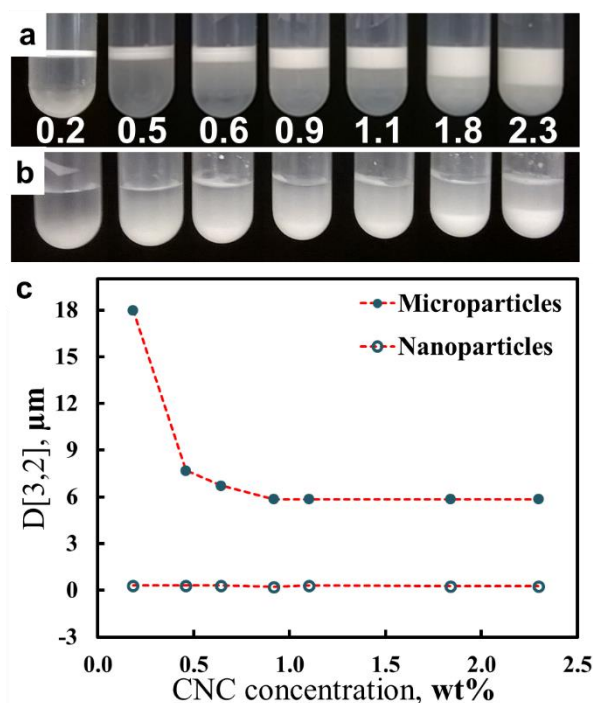


Figure 3. Photographs of (a) styrene-in-water emulsions and (b) polystyrene latex particles after polymerization, for increasing CNC concentrations ranging from 0.2 to 2.3 wt%, based on the styrene. (c) $D[3,2]$ average diameters of the two coexisting populations of polystyrene latex as a function of CNC content.

In a second step, the styrene polymerization is initiated by the hydrophobic AIBN initiator at 70°C. Two distinct populations of polystyrene particles are measured: one with $D[3,2]$ average particle diameters between 5 and 18 μm (called microparticles) and a smaller one below 1 μm (called nanoparticles) (Figure 3c). A sedimentation of the microparticles is observed because of the higher density of polystyrene ($d = 1.04 \text{ g cm}^{-3}$) compared to water (Figure 3b). Similarly to the former emulsions, the volume of the sedimented microparticles increases with increasing CNC concentration. In addition, the top aqueous phase is still cloudy suggesting the presence of polystyrene nanoparticles that are not submitted to gravity.

The polystyrene microparticles reveal a CNC concentration dependence on the diameter. The $D[3,2]$ average diameter decreased, from 18 μm down to 6 μm for CNC concentration of 0.9 wt% (Figure 3c). Above this concentration the ability of CNCs to cooperative orientation induces a densification of the CNC layer at the interface of individual droplets without diameter variation.⁵⁴ In contrast, the polystyrene nanoparticles show no dependency with CNC concentration with a $D[3,2]$ average diameter of polystyrene nanoparticles approximately 300 nm for all CNC concentrations (Figure 3c). However, it should be noticed that the CNC concentration influences the amount of nanoparticles. When increasing content of CNCs is added, more nanoparticles are observed by a very clear increase in the relative granulometry peak area without noticeable

modification of the average particle diameter (Figure S5). Another remarkable aspect is that, after polymerization, the resulting polystyrene nanoparticles ($D[3,2] = \sim 300 \text{ nm}$) are smaller than the initial styrene nanometric droplets ($D_n = 600 \text{ nm}$). The latex dispersion and the organization of CNCs at the interface were both analyzed by the visualization of detailed surfaces with scanning electron microscopy (SEM). In order to separate the two populations of polystyrene particles, the final latex dispersion was centrifuged. SEM images of the polystyrene microparticles are shown in Figure 4. The comparison of microparticles produced at two CNC concentrations shows that the microparticle diameters decrease from 10 μm to 5 μm with increasing CNC concentrations from 0.5 to 2 wt% based on styrene. Moreover, a scan of the surface of the microparticles shows that, increasing the amount of CNC introduced, the nanocrystals are densely organized along the surface of the micrometric beads (Figure 4b and Figure 4d).

SEM observation of polystyrene nanoparticles with diameters ranging from 100 to 600 nm is displayed in Figure 5. A much lower surface coverage is observed compared to microparticles. However, the presence of CNCs strongly adhering to and curved along the nanoparticle surface was clearly revealed, confirming the assumption that the styrene nanometric droplets were effectively stabilized by the CNCs. The polystyrene nanoparticles exhibit average diameters of between 100 and

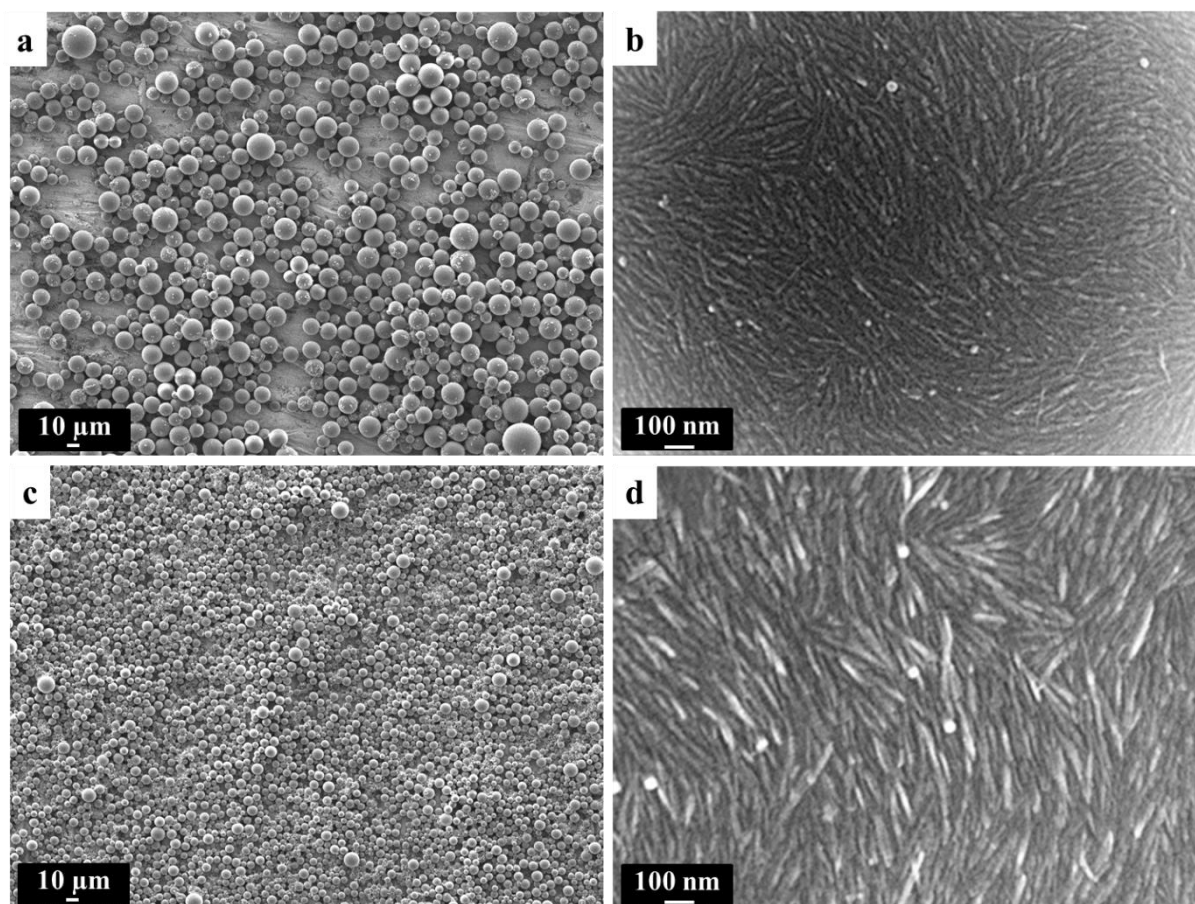


Figure 4. SEM images of microparticles polymerized from emulsions stabilized by CNCs at (a, b) 0.5 wt% and (c, d) 2 wt% based on the styrene.

400 nm, sizes close to the CNC length, which suggests an impressive bending of CNCs. The plastic deformation limits of CNCs were studied in a simulation study done by Chen et al.⁶⁷ They demonstrated that CNCs are able to bend up to a critical bending angle of approximately 60° with a greater elastic limit displacement along the (200) crystalline plane. This assumption makes it possible to hypothesize the stabilization of these

dextran to reverse the viscosity ratio between the continuous and the dispersed phase. The droplet size distributions of the resulting emulsions are represented in Figure 6 for the different viscosities. All of the curves are superimposed with the same average droplet diameter of 5 μm for the investigated viscosity ratios. Even when the continuous phase presents a viscosity three times greater than the one of the dispersed phase, it is

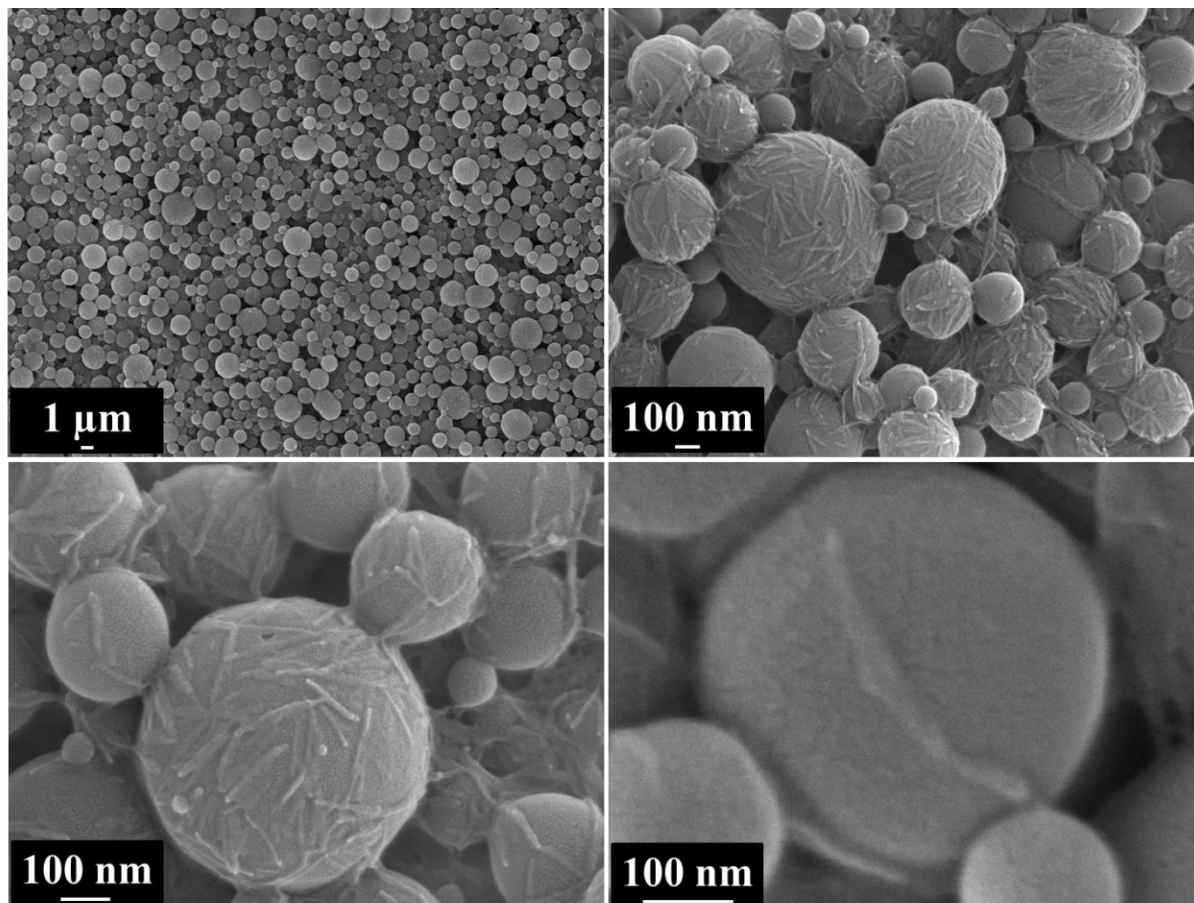


Figure 5. Representative SEM images of polystyrene nanoparticles stabilized by CNCs.

nanolatexes.

In previous studies,^{50, 51} a detailed characterization of hexadecane-in-water emulsions stabilized by unmodified CNCs showed that it was not possible to stabilize droplets smaller than 5 μm, even using ultra high shear like ultrasonication. Submicrometer droplets ($D[3,2] = 300$ nm) could be obtained only by repeated passes through a high-pressure homogenizer,⁵³ for which high-energy consumption is required. To better understand the presence of nanometric droplets in the emulsions and the presence of polystyrene nanoparticles after polymerization, several parameters were investigated. We first investigated the effect of the viscosity ratio between both phases. In contrast to hexadecane (3.5 mPa·s), styrene viscosity (0.763 mPa·s) is lower than water viscosity (1 mPa·s). The low viscosity of the dispersed phase compared to the continuous phase could result in a better deformation, which would make the stabilization of smaller droplets possible. In order to confirm this hypothesis, hexadecane-in-water emulsions were prepared with a continuous aqueous phase of higher viscosity by adding

not possible to stabilize smaller nanometric droplets. Similarly to the viscosity ratio, the variation in surface charge density showed no modification in the formation of nanometric droplets when comparing CNCs at 0.2 and 0.6 e·nm⁻² (Figure S6).

Since the adjustment of viscosity or the surface charge density of CNCs has no effect on the droplet size of hexadecane-in-water emulsion, the presence of small droplets in styrene-in-water emulsions might be ascribed to a higher concentration limit of solubility in water. In order to investigate the effect of this parameter, the next part of this study is devoted to the

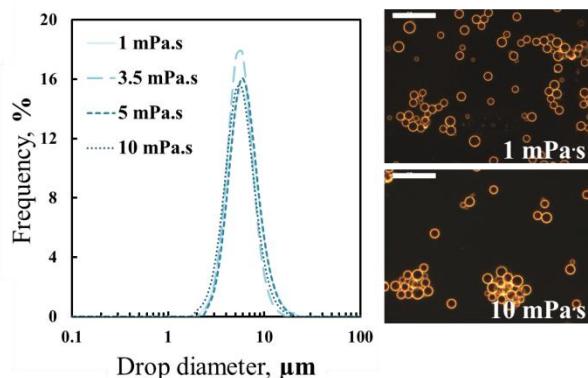


Figure 6. Droplet size distributions of emulsions stabilized with CNC at 2 wt%, based on hexadecane (3.5 mPa.s) with different aqueous phase viscosities. Optical microscopy images of emulsions. The scale bar is 50 μm .

polymerization in aqueous dispersed media of different monomers with various limits of solubility in water.

Role of the monomer on droplet and particle sizes

Unlike hexadecane, which is completely non-soluble in water, styrene has a solubility of 0.05 $\text{g}\cdot\text{L}^{-1}$ in water (Table 1). It is known that the solubility limit of styrene in water allows the nucleation of emulsion polymerization in the aqueous phase

and the further polymerization step by diffusion of monomers through the continuous phase from monomer droplets to the growing particles.⁶⁸ This ability to diffuse through the water could explain the presence of stable nanometric droplets without a high coverage of CNCs. To verify this hypothesis, the styrene was replaced by other monomers with different values of water solubility (Table 1).

The same procedure was carried out for the preparation of emulsions stabilized with CNCs and their subsequent polymerization. The resulting monomer-in-water emulsions were visualized by optical microscopy and compared to hexadecane-in-water emulsions for a concentration of CNC of 2.3 wt% (Figure 7). The $D[3,2]$ average droplet diameter of emulsions and the $D[3,2]$ average particle diameter of latex dispersions are represented in Figure 8.

We first analyzed the liquid monomer-in-water emulsions. Similarly to hexadecane, lauryl methacrylate (LMA) is insoluble in water, while isobornyl acrylate (iBoA) shows solubility in water ranging between lauryl methacrylate and styrene (Table 1). For these both monomers, CNC stabilized only micrometric liquid droplets with $D[3,2]$ average diameter of 5 μm , in the absence of nanometric droplets (Figure 7 and Figure 8).

Concerning styrene emulsions, the measurement by granulometry corroborates the results obtained by microscopy since two populations of droplets are observed: (i) a population of nanometric droplets with a diameter distribution ranging from 500 nm to 2 μm for all CNC concentrations; and (ii) a second distribution of micrometric droplets for which the diameter decreases with CNC concentration and reaches a minimum value of 5 μm for the highest CNC concentrations (Figure 7 and Figure 8).

Table 1. Monomer solubility in water, size of the droplets, initiator used size of the solid particles formed and their nomenclature and polymerization mechanisms.

Monomer	Solubility in water ($\text{g}\cdot\text{L}^{-1}$)	$D[3,2]_{\text{drop}}$	Initiator	$D[3,2]_{\text{particle}}$	Name of latex particle	Polymerization process
LMA	Insoluble	5 μm	AIBN	5 μm	Microparticle	Suspension polymerization
iBoA	0.02	5-7 μm	AIBN	5-7 μm	Microparticle	Suspension polymerization
				300 nm (<i>minor population</i>)	Nanoparticle	Emulsion polymerization
iBoA	0.02	5-7 μm	AIBN + ACPA	5-7 μm	Microparticle	Suspension polymerization
				300 nm (<i>major population</i>)	Nanoparticle	Emulsion polymerization
Styrene	0.05	5-7 μm	AIBN	5-7 μm	Microparticle	Suspension polymerization

		0.5-2 μm		300 nm (<i>major population</i>)	Nanoparticle	Emulsion polymerization
BMA	0.20	70 μm	AIBN	70 μm	Microparticle	Suspension polymerization
		1-10 μm		1-10 μm	Microparticle	Suspension polymerization
MMA	15.30	No emulsion				

The *n*-butyl methacrylate (BMA) is associated with a water solubility limit that is four times higher than styrene (Figure 8). BMA also forms emulsions with two populations of droplets (Figure 7). The granulometric characterization showed one population of droplets with diameters greater than 20 μm and another with diameters of around 1 μm (Figure 8). However, the resulting systems are unstable and the continuous and dispersed phases can mix over several hours. Finally, the water solubility of methyl methacrylate (MMA) is too high, preventing the formation of any emulsions in similar experimental conditions. The size distribution of monomer droplet is thus related to the level of the concentration limit of water solubility

of the monomer dispersed phase. When the monomer is completely insoluble in water, like in emulsions prepared with LMA or iBoA, only micrometric droplets were produced using direct sonication. Sonication produces a much larger area of the monomer/water interface than can potentially be covered by the CNCs. When sonication is stopped, the partially unprotected droplets coalesce. This coalescence results in a decrease of the oil/water interface and stops as soon as the interface is sufficiently covered. However, in the case of partial solubility in water, like with styrene, the monomer is able to diffuse through the continuous phase and thus allows the formation of nanometric droplets. The steric repulsion between CNCs avoids the coalescence of both the droplets and nanometric droplets. These results slightly differ from those reported by Zhang *et al.*⁶³ who chemically modified CNCs to increase their hydrophobicity and used them to stabilize styrene droplets of a few hundred nanometers. The authors justified the stabilization by the reduction of the interfacial tension between the styrene and the water phase due to CNC surface modification.

The waterborne latex particles were formed by polymerization of the initial emulsions by different heterogeneous polymerization mechanisms according to the water solubility of the monomers. In the case of LMA, the polymerization initiated by hydrophobic AIBN mainly occurs via a suspension polymerization process. The nucleation of suspension polymerization takes place in the monomer droplets, and the solid particles are the exact replicas of the LMA emulsion droplets (Figure 8). The SEM analysis of PLMA particles was not possible since the glass transition temperature of the polymer is too low ($T_g = -65^\circ\text{C}$), preventing formation of a solid bead for imaging. It should be observed that granulometry did not reveal the concomitant formation of PLMA nanoparticles in the final latex. In the case of the iBoA polymerization, the polymer microparticles were the replica of the micrometric droplets with a diameter of 5 μm , suggesting also a suspension polymerization mechanism initiated by the hydrophobic AIBN initiator. However, a second population of polymer nanoparticles appeared for the highest concentration of CNCs (2.3 wt%) (Figure 8). These nanoparticles were produced during the iBoA polymerization, and SEM images of P(iBoA) nanoparticles confirmed the presence of CNCs at their surface (Figure S7). The presence of both P(iBoA) microparticles and nanoparticles suggests a concomitant suspension and emulsion polymerization mechanism. The iBoA micrometric droplets were nucleated by the hydrophobic radical fragment of AIBN for suspension polymerization, leading to the production of microparticles. The formation of nanoparticles by emulsion polymerization is possible by diffusion of iBoA across the water phase towards the polymer nuclei formed by the water-soluble fraction of AIBN radical fragments. In fact, previous investigation of the emulsion polymerization initiated by the hydrophobic AIBN initiator revealed that nucleation from the fragment of AIBN in water can occur despite its low concentration in water.⁶⁸ In order to confirm the hypothesis of an emulsion polymerization mechanism, an iBoA-in-water emulsion was prepared using a mix of water-soluble/oil-soluble initiators (50:50 molar fractions of both initiators). The

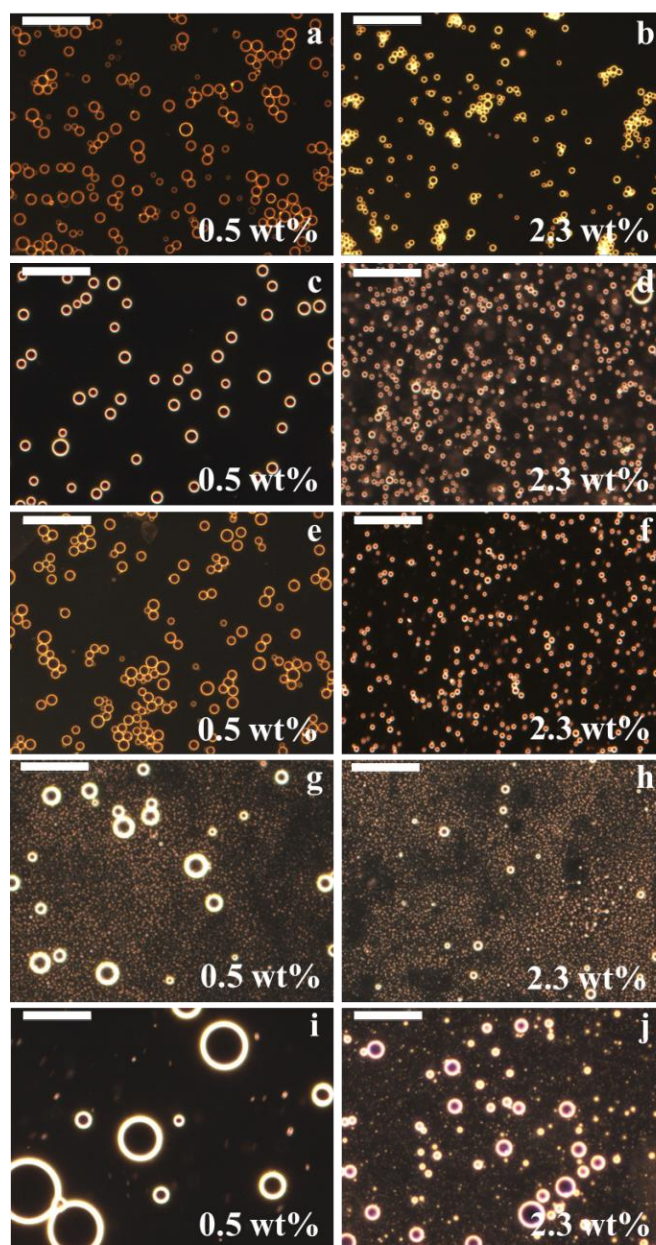


Figure 7. Optical microscopic images of emulsions of (a, b) hexadecane, (c, d) lauryl methacrylate, (e, f) isobornyl acrylate, (g, h) styrene and (i, j) butyl methacrylate in water stabilized by CNC at 0.5 wt% (left part) and 2.3 wt% (right part), based on the monomer content. The scale bar is 50 μm .

hydrophobic initiator (AIBN) was dispersed in the oil phase, whereas the water soluble initiator (4,4'-Azobis(4-cyanovaleric acid) (ACPA)) was dispersed in the aqueous phase. It should be noted that only the distribution of micrometric iBoA droplets ($\sim 5 \mu\text{m}$) was observed before polymerization. Figure 9 shows the overlay of the diameter distribution of the P(iBoA) latex particles synthesized using either both AIBN and ACPA initiators or AIBN initiators alone. When a water-soluble initiator was dissolved in the aqueous phase, more nanoparticles were

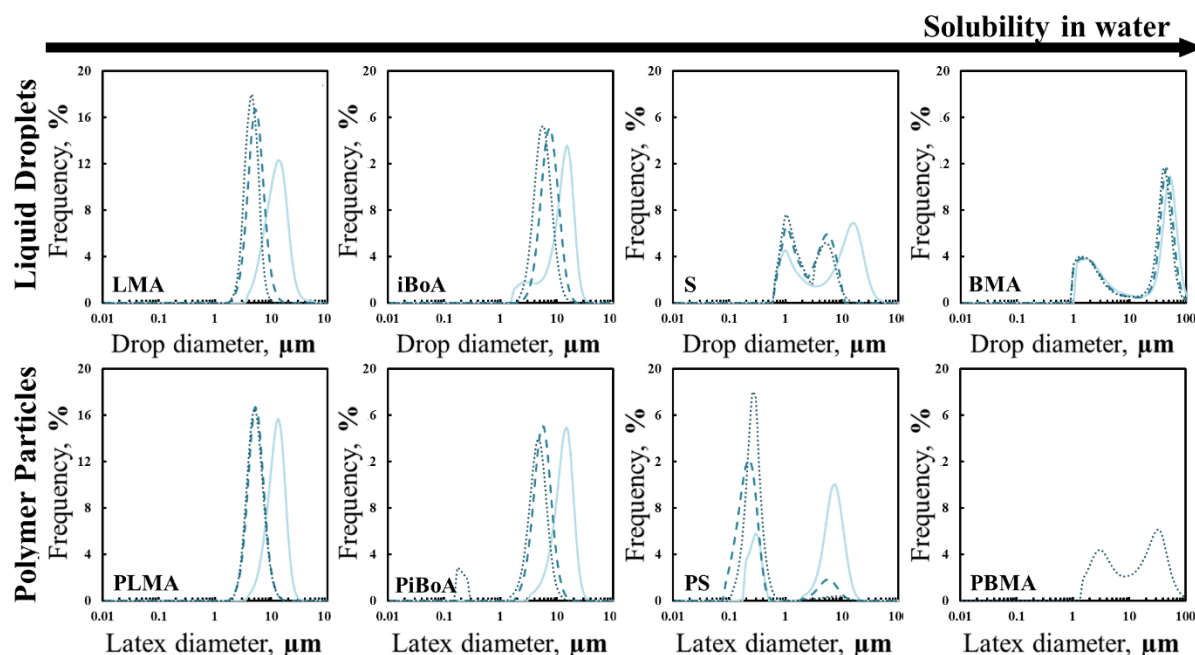


Figure 8. Droplet diameter distributions of monomer-in-water emulsions (top row) and particle size distributions of the polymerized emulsions (bottom row) for CNCs at three concentrations: 0.5 wt% (plain lines), 1 wt% (dashed lines), 2.3 wt% (dotted lines)

produced, confirming their formation by an emulsion polymerization mechanism based on a nucleation in the water phase and a diffusion of monomer from the droplets towards the growing polymer nanoparticles. Concerning styrene, the presence of both PS microparticles and nanoparticles implies, as in the case of iBoA, concomitant suspension and emulsion polymerization mechanism. PS microparticles were synthesized by a suspension polymerization mechanism initiated by the hydrophobic AIBN initiator, whereas PS nanoparticles were produced by emulsion polymerization. The population of PS nanoparticles exhibits an average diameter of 300 nm for all CNC concentrations, which is clearly lower than the diameter of the nanometric styrene droplets (0.5–2 μm). The reduction in particle size with respect to the droplet size (see Table 1 and Figure 8) confirms the diffusion of styrene from the droplets towards the growing PS nanoparticles during the polymerization process. Furthermore, the fraction of PS nanoparticles is enhanced with increasing the concentration of CNC, leading to larger PS specific surface. In summary, the emulsion polymerization mechanism, based on a nucleation in the water phase, is possible if the solubility of monomers in water allows their diffusion across the continuous phase. In the case of n-butyl methacrylate (BMA) monomer with higher limit concentration of solubility in water (Table 1), the polymerization was possible only for the highest concentration of CNCs (2.3 wt%) (Figure 8). After polymerization, only PBMA microparticles were observed as the replica of the BMA droplets, suggesting a suspension polymerization mechanism initiated by the hydrophobic AIBN initiator.

In a previous work of Werner *et al.*⁶⁴, the authors studied the preparation of latexes using acetylated CNCs. They ascribed the production of polystyrene nanoparticles, concomitantly to the production of microparticles, to the extrusion of styrene

monomer from the droplets and its polymerization in the continuous water phase initiated by isolated CNCs acting as nucleation sites. We showed that, in our case, nanometric droplets are already present in the starting styrene-in-water emulsion. The authors also suggested that the extrusion was due to incomplete coverage of the droplets that could be avoided by aggregation conditions such as the addition of salt. However, in this study, polystyrene nanoparticles were produced on a large range of coverage of the emulsion droplets, and notably above the limited coalescence domain in the presence of salt, and styrene nanoparticles can even be

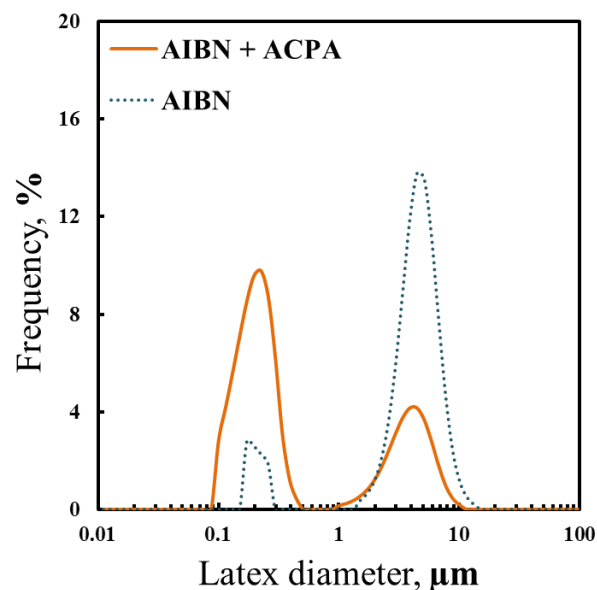


Figure 9. Latex size distributions of the polymerized emulsions stabilized by CNC at 2.3 wt% based on isobornyl acrylate using AIBN and AIBN/ACPA as initiators.

prepared in the higher coverage conditions. Furthermore, CNCs were identified as nucleation sites in the aqueous phase, whereas we previously confirmed the absence of CNCs in the aqueous phase by titration for emulsions prepared under similar conditions.^{50, 51}

In this study, we highlighted that droplets can be prepared from a large range of monomers, leading to latex particles made of polymers of a wide range of glass transition temperatures (T_g , $T_{g, PLMA} \sim -65$ °C, $T_{g, PBMA} \sim 20$ °C, $T_{g, PiBoA, PS} \sim 100$ °C).⁶⁹ We revealed the clear impact of the limit concentration of water solubility of the monomer on the process of particle formation for their polymerization in aqueous dispersed media. (1) The more hydrophobic monomer, LMA, is not able to diffuse through the water phase and thus produces polymer microparticles by suspension polymerization as replicas of the initial micrometric droplets. (2) In the case of monomers with intermediate limit solubility in water, like iBoA, only micrometric droplets are obtained (like LMA). However particle formation takes place through two polymerization mechanisms: microparticles were obtained by suspension polymerization, and nanoparticles were produced by emulsion polymerization. The emulsion polymerization mechanism is possible due to the partial solubility of the monomer in water that allows its diffusion through the continuous phase and its nucleation induced by the fraction of AIBN that can be dissolved in water.⁶⁸ (3) Monomers with partial solubility in water, like styrene, allow the stabilization of emulsions with initial micro and nanometric droplets. The two concomitant mechanisms of suspension and emulsion polymerization produce microparticles and nanoparticles from the emulsion droplets. (4) By increasing again the solubility in water, like for BMA monomer, unstable liquid emulsion containing only large monomer droplets can be processed, leading to the formation of large PBMA particles with diameter far above 1 μm , in the absence of nanoparticles. (5) For very polar monomers, like MMA, associated with a high solubility in water, the formation of emulsions is even not possible.

Conclusions

This study reports the efficiency of unmodified CNCs to act as stabilizer of both monomer-in-water Pickering emulsion and nanocomposite latex particles with controlled dimensions. Styrene-in-water emulsions have two populations of droplets: (i) micrometric droplets with diameters that decrease with CNC concentration and that reach a minimum value of 5 μm for the highest CNC concentrations and (ii) nanometric droplets with a diameter distribution ranging from 500 nm to 2 μm for all CNC concentrations. The polymerization of the initial styrene-in-water Pickering emulsions produced waterborne polystyrene latexes through two concomitant mechanisms: (i) microparticles were obtained by suspension polymerization mechanism initiated by the hydrophobic AIBN initiator and (ii) nanoparticles were produced by emulsion polymerization mechanism initiated by polymer nuclei formed by the water-soluble fraction of AIBN radical fragments.

Through the polymerization of a range of vinylic monomers (LMA, iBoA, S and BMA), we confirmed that the balance between the micro- and nanoparticles of latex are driven by the ability of the monomer to diffuse across the water phase related to its limit concentration of solubility in water. We therefore demonstrated that the solubility of the monomer in water is a key parameter for designing Pickering polymer nanoparticles. Furthermore, CNC efficiently stabilize such interface and increasing the concentration of CNC allows the stabilization of a larger number of styrene droplets, which results in a larger fraction of nanoparticles. The range of waterborne latex (PLMA, PiBoA, PS, PBMA) with various glass transition temperatures and final particle sizes produced by surfactant-free polymerization in aqueous dispersed media from unmodified CNCs offers new perspectives to design CNC-reinforced polymer materials.

Conflicts of interest

There are no conflicts to declare

Acknowledgements

This work was carried out within the framework of the French National Research Agency (ANR Project CE08 2015). We gratefully acknowledge Emilie Perrin and Joëlle Davy (INRA, Nantes, France) for their excellent technical assistance for TEM and SEM visualizations, as well as Nicolas Stephant (Institut des Matériaux Jean Rouxel, Université de Nantes) for access to the SEM equipment. We are equally grateful to Geneviève Llamas (INRA, Nantes, France) for her support in laser scattering particle size analysis and Matthieu Tetart for the preparation of samples.

Notes and references

1. B. G. Rånby, A. Banderet and L. G. Sillén, *Acta Chemica Scandinavica*, 1949, **3**, 649-650.
2. B. G. Rånby, *Discuss. Faraday Soc.*, 1951, **11**, 158-164.
3. R. H. Marchessault, F. F. Morehead and N. M. Walter, 1959.
4. R. H. Marchessault, F. F. Morehead and M. J. Koch, *Journal of Colloid Science*, 1961, **16**, 327-344.
5. J. F. Revol, H. Bradford, J. Giasson, R. H. Marchessault and D. G. Gray, *International Journal of Biological Macromolecules*, 1992, **14**, 170-172.
6. V. Favier, H. Chanzy and J. Y. Cavaille, *Macromolecules*, 1995, **28**, 6365-6367.
7. X. M. Dong, J.-F. Revol and D. G. Gray, *Cellulose*, 1998, **5**, 19-32.
8. M. M. de Souza Lima and R. Borsali, *Langmuir*, 2002, **18**, 992-996.
9. O. Nechyporchuk, M. N. Belgacem and J. Bras, *Industrial Crops and Products*, 2016, DOI: 10.1016/j.indcrop.2016.02.016.
10. A. Dufresne, *Journal*, 2013.

11. S. J. Eichhorn, C. A. Baillie, N. Zafeiropoulos, L. Y. Mwaikambo, M. P. Ansell, A. Dufresne, K. M. Entwistle, P. J. Herrera-Franco, G. C. Escamilla, L. Groom, M. Hughes, C. Hill, T. G. Rials and P. M. Wild, *Journal of Materials Science*, 2001, **36**, 2107-2131.
12. O. Nechyporchuk, M. N. Belgacem and J. Bras, *Industrial Crops and Products*, 2016, **93**, 2-25.
13. E. J. Foster, R. J. Moon, U. P. Agarwal, M. J. Bortner, J. Bras, S. Camarero-Espinosa, K. J. Chan, M. J. D. Clift, E. D. Cranston and S. J. Eichhorn, *Chemical Society Reviews*, 2018, **47**, 2609-2679.
14. A. Dufresne, *Current Opinion in Colloid & Interface Science*, 2017, **29**, 1-8.
15. Y. Habibi, *Chemical Society Reviews*, 2014, **43**, 1519-1542.
16. W. J. Grigsby, C. J. Ferguson, R. A. Franich and G. T. Russell, *International journal of adhesion and adhesives*, 2005, **25**, 127-137.
17. L. N. Butler, C. M. Fellows and R. G. Gilbert, *Progress in Organic Coatings*, 2005, **53**, 112-118.
18. J. Zhang, X. Li, X. Shi, M. Hua, X. Zhou and X. Wang, *Progress in Natural Science: Materials International*, 2012, **22**, 71-78.
19. J. M. Asua, *Prog. Polym. Sci.*, 2002, **27**, 1283-1346.
20. C. S. Chern, *Prog. Polym. Sci.*, 2006, **31**, 443-486.
21. S. Kawaguchi and K. Ito, in *Polymer Particles*, ed. M. Okubo, Springer-Verlag Berlin, Berlin, 2005, vol. 175, pp. 299-328.
22. G. W. Ceska, *Journal of Applied Polymer Science*, 1974, **18**, 427-437.
23. K. Tauer, R. Deckwer, I. Kühn and C. Schellenberg, *Colloid & Polymer Science*, 1999, **277**, 607-626.
24. U. Yildiz, B. Hazer and K. Tauer, *Polymer Chemistry*, 2012, **3**, 1107-1118.
25. M. Save, M. Manguian, C. Chassenieux and B. Charleux, *Macromolecules*, 2005, **38**, 280-289.
26. L. Houillot, J. Nicolas, M. Save, B. Charleux, Y. T. Li and S. P. Armes, *Langmuir*, 2005, **21**, 6726-6733.
27. Z. F. Liu, H. N. Xiao, N. Wiseman and A. Zheng, *Colloid and Polymer Science*, 2003, **281**, 815-822.
28. H. Ahmad and K. Tauer, *Macromolecules*, 2003, **36**, 648-653.
29. G. Riess and C. Labbe, *Macromol. Rapid Commun.*, 2004, **25**, 401-435.
30. C. J. Ferguson, R. J. Hughes, B. T. T. Pham, B. S. Hawket, R. G. Gilbert, A. K. Serelis and C. H. Such, *Macromolecules*, 2002, **35**, 9243-9245.
31. G. Delaittre, J. Nicolas, C. Lefay, M. Save and B. Charleux, *Chem Commun (Camb)*, 2005, DOI: 10.1039/b415959d, 614-616.
32. B. Charleux, G. Delaittre, J. Rieger and F. D'Agosto, *Macromolecules*, 2012, **45**, 6753-6765.
33. S. L. Canning, G. N. Smith and S. P. Armes, *Macromolecules*, 2016, **49**, 1985-2001.
34. I. Martin-Fabiani, J. L. de la Haye, M. Schulz, Y. Liu, M. Lee, B. Duffy, F. D'Agosto, M. Lansalot and J. L. Keddie, *ACS Appl. Mater. Interfaces*, 2018, **10**, 11221-11232.
35. J. H. Zhou, H. T. Yao and J. Z. Ma, *Polymer Chemistry*, 2018, **9**, 2532-2561.
36. J. Bernard, M. Save, B. Arathoon and B. Charleux, *Journal of Polymer Science Part a-Polymer Chemistry*, 2008, **46**, 2845-2857.
37. F. L. Hatton, M. Ruda, M. Lansalot, F. D'Agosto, E. Malmstrom and A. Carlmark, *Biomacromolecules*, 2016, **17**, 1414-1424.
38. K. Ferji, P. Venturini, F. Cleymand, C. Chassenieux and J. Six, *Polym. Chem.*, 2018, 2868-2872.
39. W. Ramsden, *Proceedings of the royal Society of London*, 1903, **72**, 156-164.
40. S. U. Pickering, *Journal of the Chemical Society, Transactions*, 1907, **91**, 2001-2021.
41. I. Capron, O. J. Rojas and R. Bordes, *Current opinion in colloid and interface science*, 2017, **29**, 83-95.
42. A. Schrade, K. Landfester and U. Ziener, *Chemical Society Reviews*, 2013, **42**, 6823-6839.
43. M. Percy, C. Barthet, J. Lobb, M. Khan, S. Lascelles, M. Vamvakaki and S. Armes, *Langmuir*, 2000, **16**, 6913-6920.
44. J. H. Chen, C.-Y. Cheng, W.-Y. Chiu, C.-F. Lee and N.-Y. Liang, *European Polymer Journal*, 2008, **44**, 3271-3279.
45. X. Song, Y. Zhao, H. Wang and Q. Du, *Langmuir*, 2009, **25**, 4443-4449.
46. M. M. Gudarzi and F. Sharif, *Soft Matter*, 2011, **7**, 3432-3440.
47. B. Brunier, N. Sheibat-Othman, M. Chniguir, Y. Chevalier and E. Bourgeat-Lami, *Langmuir*, 2016, **32**, 6046-6057.
48. L. Delafresnaye, P.-Y. Dugas, P.-E. Dufils, I. Chaduc, J. Vinas, M. Lansalot and E. Bourgeat-Lami, *Polymer Chemistry*, 2017, **8**, 6217-6232.
49. K. P. Oza and S. G. Frank, *Journal of Dispersion Science and Technology*, 1986, **7**, 543-561.
50. I. Kalashnikova, H. Bizot, B. Cathala and I. Capron, *Langmuir*, 2011, **27**, 7471-7479.
51. I. Kalashnikova, H. Bizot, P. Bertoncini, B. Cathala and I. Capron, *Soft Matter*, 2012, **9**, 952-959.
52. M. Gestranus, P. Stenius, E. Kontturi, J. Sjöblom and T. Tammelin, *Colloids and Surfaces A: Physicochemical and Engineering Aspects*, 2017, **519**, 60-70.
53. C. Jimenez Saelices and I. Capron, *Biomacromolecules*, 2018, **19**, 460-469.
54. F. Cherhal, F. Cousin and I. Capron, *Biomacromolecules*, 2016, **17**, 496-502.
55. Z. Dastjerdi, E. D. Cranston and M. A. Dubé, *International Journal of Adhesion and Adhesives*, 2018, **81**, 36-42.
56. A. B. Elmabrouk, T. Wim, A. Dufresne and S. Boufi, *Journal of applied polymer science*, 2009, **114**, 2946-2955.
57. A. Ben Mabrouk, H. Kaddami, A. Magnin, M. N. Belgacem, A. Dufresne and S. Boufi, *Polymer Engineering & Science*, 2011, **51**, 62-70.
58. A. B. Mabrouk, A. Magnin, M. N. Belgacem and S. Boufi, *Composites Science and Technology*, 2011, **71**, 818-827.
59. A. B. Mabrouk, M. R. Vilar, A. Magnin, M. N. Belgacem and S. Boufi, *Journal of Colloid and Interface Science*, 2011, **363**, 129-136.
60. S. A. Kedzior, H. S. Marway and E. D. Cranston, *Macromolecules*, 2017, **50**, 2645-2655.

61. W. Du, J. Guo, H. Li and Y. Gao, *ACS Sustainable Chem. Eng.*, 2017, **5**, 7514-7523.
62. S. A. Kedzior, M. A. Dubé and E. D. Cranston, *ACS Sustainable Chem. Eng.*, 2017, **5**, 10509-10517.
63. Y. Zhang, V. Karimkhani, B. T. Makowski, G. Samaranayake and S. J. Rowan, *Macromolecules*, 2017, **50**, 6032-6042.
64. A. Werner, V. Schmitt, G. Sèbe and V. Héroguez, *Polymer Chemistry*, 2017.
65. S. Arditty, C. P. Whitby, B. P. Binks, V. Schmitt and F. Leal-Calderon, *The European Physical Journal E*, 2003, **11**, 273-281.
66. R. Aveyard, B. P. Binks and J. H. Clint, *Advances in Colloid and Interface Science*, 2003, **100**, 503-546.
67. P. Chen, Y. Ogawa, Y. Nishiyama, A. E. Ismail and K. Mazeau, *Physical Chemistry Chemical Physics*, 2016, **18**, 19880-19887.
68. C. Chern, *Progress in Polymer Science*, 2006, **31**, 443-486.
69. J. Brandrup, E. Immergut, E. A. Grulke, A. Abe and D. R. Bloch, *Polymer handbook*, 4th edn., 2003.